Published in final edited form as:

Curr Biol. 2018 April 23; 28(8): 1273–1280.e3. doi:10.1016/j.cub.2018.02.054.

Direct Control of *SPEECHLESS* by PIF4 in the High-Temperature Response of Stomatal Development

On Sun Lau[1,2,9,*], **Zhuojun Song**[1,8], **Zimin Zhou**[1,8], **Kelli A. Davies**[2], **Jessica Chang**[2,6], **Xin Yang**[1], **Shenqi Wang**[1], **Doris Lucyshyn**[3,7], **Irene Hui Zhuang Tay**[1], **Philip A. Wigge**[3,4], and **Dominique C. Bergmann**[2,5,*]

[1]Department of Biological Sciences, National University of Singapore, 14 Science Drive 4, Singapore 117543, Singapore

[2]Department of Biology, Stanford University, Stanford, CA 94305, USA

[3]Department of Cell and Developmental Biology, John Innes Centre, Norwich NR4 7UH, UK

[4]Sainsbury Laboratory, University of Cambridge, 47 Bateman Street, Cambridge CB2 1LR, UK

[5]Howard Hughes Medical Institute, Stanford University, Stanford, CA 94305, USA

SUMMARY

Environmental factors shape the phenotypes of multicellular organisms. The production of stomata — the epidermal pores required for gas exchange in plants—is highly plastic and provides a powerful platform to address environmental influence on cell differentiation [1-3]. Rising temperatures are already impacting plant growth, a trend expected to worsen in the near future [4]. High temperature inhibits stomatal production, but the underlying mechanism is not known [5]. Here, we show that elevated temperature suppresses the expression of SPEECHLESS (SPCH), the basic-helix-loop-helix (bHLH) transcription factor that serves as the master regulator of stomatal lineage initiation [6, 7]. Our genetic and expression analyses indicate that the suppression of *SPCH* and stomatal production is mediated by the bHLH transcription factor PHYTOCHROMEINTERACTING FACTOR 4 (PIF4), a core component of high-temperature signaling [8]. Importantly, we demonstrate that, upon exposure to high temperature, PIF4 accumulates in the stomatal precursors and binds to the promoter of *SPCH*. In addition, we find *SPCH* feeds back negatively to the *PIF4* gene. We propose a model where warm-temperature-

[*]Correspondence: onsunlau@nus.edu.sg (O.S.L.), bergmann@stanford.edu (D.C.B.).

[6]Present address: Department of Genetics, Stanford Medical School, Stanford, CA 94305, USA

[7]Present address: Department of Applied Genetics and Cell Biology, University of Natural Resources and Life Sciences, Muthgasse 18, 1190 Vienna, Austria

[8]These authors contributed equally

[9]Lead Contact

AUTHOR CONTRIBUTIONS

O.S.L. and D.C.B. conceived the study and designed the experiments. O.S.L., Z.S., Z.Z., K.A.D., X.Y., S.W., D.L., and I.H.Z.T. constructed the biological materials and performed the experiments. J.C. carried out bioinformatics analyses. O.S.L. and D.C.B. wrote the manuscript with contributions from P.A.W.

SUPPLEMENTAL INFORMATION

Supplemental Information includes four figures and two tables and can be found with this article online at https://doi.org/10.1016/j.cub.2018.02.054.

DECLARATION OF INTERESTS

The authors declare no competing interests.

activated PIF4 binds and represses *SPCH* expression to restrict stomatal production at elevated temperatures. Our work identifies a molecular link connecting high-temperature signaling and stomatal development and reveals a direct mechanism by which production of a specific cell lineage can be controlled by a broadly expressed environmental signaling factor.

Graphical Abstract

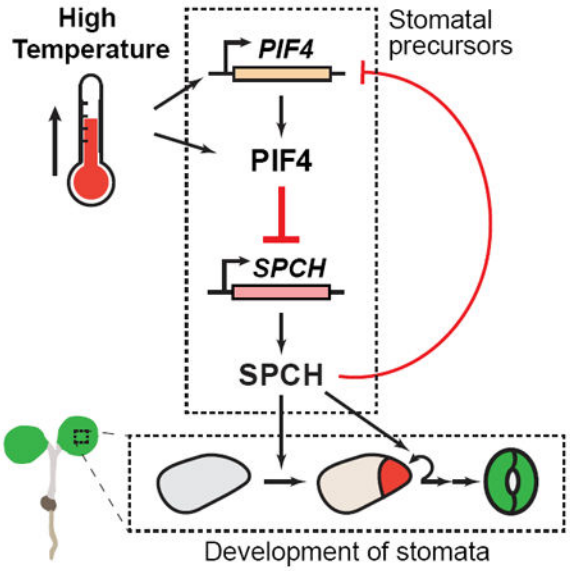

RESULTS

High-Temperature Control of Stomatal Development Involves the Suppression of *SPEECHLESS*

Temperature is a major environmental cue sensed by plants. In *Arabidopsis*, elevated ambient temperatures of 28°C–30°C induce a suite of developmental and morphological changes, including organ elongation, early flowering, and reduced stomatal production (Figure 1B) [5, 8-10]. Due to the documented increase in global temperatures, efforts to understand these processes at the molecular level are growing, and the impact of the stomatal high-temperature response is particularly significant because changes in the number of stomata—the sites for evapotranspiration—will likely influence high temperature and drought tolerance in plants [11]. In addition, given the role of stomata in the global water cycle, this developmental response in land plants may play a part in influencing global climate [12].

Stomata are one of the final products of a specialized epidermal lineage (Figure 1A) [1, 2]. In *Arabidopsis*, precursor cells of the stomatal lineage, meristemoid mother cells (MMCs), and meristemoids possess self-renewing properties, and the activity of these precursors provides flexibility in the number and ratio of stomatal and non-stomatal epidermal cells produced. The initiation and proliferation of stomatal precursors is driven by the master transcription factor SPEECHLESS (SPCH), which regulates hundreds of genes to promote divisions and fate transitions [6, 7, 13]. SPCH also acts as a key regulatory node that allows

developmental and external signals to influence the activity of the lineage. SPCH protein is targeted by components of the MITOGEN-ACTIVATED PROTEIN KINASE (MAPK) and brassinosteroid (BR) signaling pathways [14-16]. Osmotic stress also appears to influence the lineage activity through MAPK-mediated regulation of SPCH [17]. Given the critical role of SPCH in controlling the stomatal lineage, we hypothesized that it may be a regulatory point for high-temperature signaling. To test this, we first examined the effect of elevated ambient temperature on *SPCH* expression by using a transcriptional reporter (*SPCHpro:nucGFP*) [6]. At standard conditions (22°C), expression of the reporter was highest in the stomatal precursors, and its intensity declined as the lineage progressed (Figure 1C). Using the same image acquisition settings, however, the reporter was expressed at lower levels and in fewer cells at elevated temperature (28°C; Figures 1D–1F; Figures S1A and S1C for its effect on stomatal lineage populations and SPCH targets). These results suggest that higher temperature inhibits *SPCH* expression. We also examined the behavior of a translational reporter of *SPCH* (*SPCHpro:SPCHYFP*) and found similar downregulation of the reporter by higher temperature (Figures S1E–S1G).

Previously, SPCH was shown to be inhibited post-translationally by MAPK signaling in response to osmotic stress [17]. This conclusion was supported by monitoring a MAPK-insensitive *SPCH* reporter in which amino acid residues normally targeted by MAPKs were substituted by alanines [14] and finding that this MAPK-insensitive reporter was also insensitive to drought signals. Our MAPK-insensitive reporter (*SPCHpro:SPCH2- 4A-YFP*), consistent with previous reports, was highly expressed, and it produced excessive numbers of SPCH-expressing stomatal precursors at 22°C (Figure 1G) [14]. When grown at 28°C, however, the brightness of the reporter was dramatically reduced, as were the number of stomatal precursors expressing it (Figures 1H–1J; Figures S1B and S1D for changes in stomatal lineage populations and SPCH targets). As a control for temperature effect on yellow fluorescent protein (YFP) and gene reporters of the stomatal lineage, we analyzed another nuclear-expressed stomatal lineage protein, *CYCD7pro:-CYCD7-LGK-YFP* [18, 19]. No noticeable difference in brightness of the *CYCD7* reporter expression was observed at the two temperatures (22°C and 28°C; Figures S1H–S1J). The dramatic downregulation of even the stabilized form of SPCH protein at 28°C (Figures 1G–1J) suggests that phospho-regulation of SPCH protein may not play a significant role in the response and, together with the transcriptional reporter analysis, may hint at possible regulation at the transcriptional level. Regardless, our analyses indicate that *SPCH* is a prime regulatory node for elevated temperature control of the stomatal lineage.

PIF4 Controls the Temperature-Dependent Response in Stomatal Production

In elevated temperature signaling, PHYTOCHROME-INTERACTING FACTOR 4 (PIF4) is a central regulator that orchestrates developmental responses [8, 9]. A subset of PIF family basic-helix- loop-helix (bHLH) transcription factors are well-established repressors of light signaling [20], and through physical interaction with light-activated phytochromes, they are phosphorylated and downregulated [21-23]. Among the PIFs, however, only plants lacking *PIF4* display defects in the high-temperature response, and high temperature induces *PIF4* expression at both the transcriptional and post-transcriptional levels [8, 24]. The recent

identification of phytochromes, particularly phyB, as thermosensors further suggest PIF4 as the direct signaling component downstream of high-temperature perception [25, 26].

To investigate the potential regulatory role of *PIF4* in stomatal development, we monitored stomatal production in response to temperature in *pif4* mutants. Wild-type (WT) and two loss-offunction mutants of *PIF4, pif4*, and *pif4-2* [27, 28] were grown either continuously at standard temperature (22°C) or shifted to 28°C after seedling establishment (at four days post-germination [dpg]) under both long-day (LD) and short-day (SD) conditions. Stomatal index (SI), the ratio of stomata to all epidermal cells in a given area, was scored in mature abaxial cotyledons (14 and 27 dpg for LD and SD, respectively; plants were at similar growth stage at these time points). In WT, SI showed a significant decrease in response to the high-temperature shift at both LD and SD (Figures 2A and 2B, leftmost columns). Among the two photoperiods, the stomatal response at SD was more pronounced (Figure 2C), which is in agreement with previous findings that *PIF4*-mediated responses are often more prominent under short days [25, 29, 30]. Interestingly, the high-temperature response was almost completely absent in both *pif4* and *pif4-2* at both LD and SD (Figure 2; cell density data in Figures S2A and S2B), suggesting that *PIF4* is important in this response under both photoperiods. We also tested the stomatal response to lower temperature (12°C) in WT and *pif4* and found that low temperature promotes stomatal production (i.e., leads to an increase in stomatal index; Figure S2C). In contrast to the response at higher temperatures, however, SI of WT and *pif4* at 12°C was not significantly different, which indicates a reduced influence of *PIF4* at low temperature. Collectively, our mutant analyses demonstrate a critical role of *PIF4* in the stomatal developmental response toward high temperature.

PIF4 Is Expressed in Stomatal Precursors and Regulates *SPCH* Expression

We next asked how *PIF4* may influence *SPCH* and the stomatal precursors in response to high temperature. A previous study on phyB demonstrated that its targeted expression both within and outside of the stomatal lineage (i.e., in mesophyll and phloem) in *phyB* mutants is sufficient to restore proper lightdependent stomatal development, suggesting phyB signaling can operate both cell autonomously and systemically [31]. Thus, as a signaling component downstream of phyB, PIF4 could conceivably also function within the stomatal lineage. A reporter of PIF4 protein expression (*PIF4pro:PIF4-GFP*) was expressed in the nucleus of the stomatal precursor cells (Figure 3A, marked with asterisks) after plants were transferred to 28°C (16 hr) to enhance *PIF4* expression [8, 32]. Interestingly, at standard temperature (22°C), the *PIF4* reporter was undetectable in the stomatal lineage (Figure 3B), suggesting that high temperature promotes PIF4 accumulation in the stomatal precursors.

Because PIF4 is a transcriptional regulator present in the stomatal lineage at high temperature, a reasonable hypothesis is that it mediates the high-temperature suppression of *SPCH*. We monitored *SPCH* transcript accumulation in seedlings with altered PIF4 levels by qRT-PCR (Figure 3C). Consistent with our analysis of the *SPCH* reporter (Figures 1C and 1D), *SPCH* transcript decreased in WT in response to high temperature (Figure 3C, leftmost columns). In *pif4*, however, high-temperature repression was diminished. Moreover, the overall level and pattern of *SPCH* expression in WT and *pif4* in response to high

temperature correlates with stomatal production (compare Figure 3C with Figure 2A). Conversely, overexpression of *PIF4* (*PIF4-OX*) [32] resulted in low levels of *SPCH* expression and the effect of high temperature was also reduced (Figure 3C, rightmost column). Thus, the expression analyses show that *PIF4* plays a role in suppressing *SPCH* expression at high temperature.

PIF4 Binds to *SPCH* Promoter in a Temperature-Dependent Manner

Our sequence analysis identified six E-boxes (CANNTG), the DNA elements that bHLHs like PIF4 typically bind [33], in the promoter of *SPCH* (Figure 3D). To test the association between PIF4 and the *SPCH* gene, we utilized the highly sensitive maximized objects for better enrichment-chromatin immunoprecipitation (MOBE-ChIP) method, which has enabled us to detect stomatal lineage-specific protein-DNA interactions [13, 19, 34]. A transgenic line expressing Myc-tagged PIF4 natively (*PIF4pro:PIF4-MYC*) was used [32] and, following protocols from previous studies that showed the temperature dependency of PIF4 binding [10, 35], subjected to a temperature shift regime from 12°C to 28°C. We observed a considerable enrichment of PIF4 at the promoter regions of *SPCH*, corresponding to the location of the E-boxes (P1–P3), in high-temperature- treated *PIF4-MYC* (Figures 3D and 3E, red columns). Importantly, no substantial enrichment was found in regions that are further up- (5′ and 5″) or downstream (3′) of the binding regions, and the promoter regions were not enriched in nontreated *PIF4-MYC* and WT samples. The temperature-dependent binding of PIF4 may be due to an increase in PIF4 abundance at high temperature as reported previously [32] and/or the enrichment within the stomatal precursor cells (Figure 3A). It is worth noting that standard ChIP assays yielded only weak enrichment of PIF4 on the *SPCH* promoter (Figure S3). Because genomic regions of *SPCH* are likely condensed and inaccessible in non-stomatal lineage cells [36], only the pool of PIF4 expressed in stomatal precursors is expected to bind *SPCH*, thus requiring MOBE-ChIP sensitivity for detection.

Feedback Regulation of *PIF4*-Mediated Stomatal Control by SPCH

Our previous genome-wide characterization of SPCH targets revealed an enrichment of genes involved in diverse environmental and hormone pathways, suggesting a complex interplay between SPCH and these pathways [13]. For example, SPCH, which is regulated by BR signaling, also directly binds and regulates key genes involved in BR biosynthesis and signaling [13, 15]. We investigated whether a similar feedback regulatory mechanism exists between *SPCH* and *PIF4* in the thermal response. The ChIP sequencing (ChIP-seq) profile of SPCH at the promoter region of *PIF4* showed a clear enrichment (Figure 4A), and there was a modest expression response of *PIF4* to SPCH induction [13]. Because SPCH is restricted to the stomatal precursors in the epidermis [37] and the previous RNA-seq dataset was based on broad induction, we improved specificity and sensitivity of the assay by creating an epidermal specific steroid-inducible gene expression system to rapidly activate *SPCH* activity in the relevant cells [38]. Briefly, a stabilized form of SPCH was fused with the glucocorticoid receptor (GR), which holds it inactive in the cytoplasm until application of dexamethasone (DEX), and expressed under the epidermalspecific *ATML1* promoter. Samples for RNA-seq were collected at 0 and 12 hr, and four replicates of each genotype (*ATML1p:SPCH1-4A-GR* and WT) were used to increase the statistical power to detect

modest expression changes. Using this epidermal system, we found *PIF4* to be significantly downregulated upon induction of SPCH (Figure 4B; Table S1). As controls, stomatal lineage targets previously shown to be upregulated upon SPCH induction (*ICE1* and *ERL1*) were also upregulated in this dataset. These results suggest that SPCH directly binds *PIF4* and represses its expression, potentially forming a negative feedback loop with *PIF4*.

DISCUSSION

We have identified a molecular link that connects high-temperature signaling to stomatal development. Based on our data, we propose a working model where high temperature suppresses stomatal development through repressing *SPCH* expression, which is facilitated by the high-temperature-induced binding of PIF4 to *SPCH* promoter sequences (Figure 4C). Transcriptional repression of *SPCH* would lead to reduced numbers and proliferative activity of the stomatal precursors, ultimately resulting in lowered production of stomatal guard cells.

The discovery of the high-temperature-induced transcriptional regulation of *SPCH* is novel, as previous works have only identified *SPCH* regulation at the protein level by external/intercellular stimuli, such as osmotic stress and BR discussed above [15-17]. The different modes of *SPCH* regulation may be attributed to the signaling mechanism of the stimuli involved. For example, BR signaling employs a cascade of kinases and phosphatases that relay signals originated from a distance to its local effectors [39]. To regulate *SPCH*, the key BR-signaling kinase BIN2 targets both the MAPK pathway that downregulates SPCH and SPCH itself [15, 16]. In contrast, accumulating evidence suggests that high-temperature signaling operates with few signaling intermediates— with PIF4, a transcription factor, being directly downstream of the thermoreceptors in controlling key genes in thermomorphogenesis [9, 25]. Our findings that PIF4 directly binds and regulates *SPCH* is thus in line with this regulatory mode of thermo-signaling. This mechanism may enable elevated temperature to influence the production of this critical cell lineage along with other growth and developmental processes in a coordinated manner.

Although another potential form of *SPCH* regulation by PIF4 is through heterodimerization of these two bHLH proteins [33], such interactions have not been reported in large-scale interactome studies [40]. Moreover, we did not detect protein-protein interactions between PIF4 and SPCH in directed yeast twohybrid assays (Figure S4). Thus, it appears unlikely that PIF4 influences SPCH activity through dimerization.

We also uncovered negative feedback regulation of the *PIF4* gene by *SPCH*, where SPCH directly binds and represses *PIF4* expression (Figure 4C). This mechanism may give rise to a switch-like behavior to the stomatal precursors such that, whereas the lineage can be repressed by high temperature, the fraction of cells that accumulate threshold levels of SPCH at high temperature can continue to accumulate SPCH (because they downregulate *PIF4*) to complete the specification process. The feedback regulation also highlights that, like other “master regulator” transcription factors (e.g., MyoD), SPCH has both activating and repressive effects on transcription. Although SPCH acts as an activator for well-known stomatal genes, such as *ICE1* and *TMM*, globally, a smaller but significant percentage of

SPCH-binding targets were shown to be repressed upon SPCH induction [13]. One potential mechanism may be through the assembly of complexes containing different partners depending on the developmental or environmental context, and in the future, these complexes can be pursued through immunoprecipitation of SPCH followed by mass spectrometry for peptide identification.

Because PIF4 acts as a repressor in light signal transduction and is regulated by hormone signaling, our findings prompt the question of whether PIF4 or its homologs also regulate stomatal development in response to light and hormones using similar strategies. A previous study provided genetic evidence supporting the involvement of *PIF4* in the light-mediated control of stomatal development [41]. Intriguingly, in contrast to the negative effect on stomatal development shown here, *PIF4* appears to act positively to promote stomatal production under light. This discrepancy suggests that *PIF4* may influence the stomatal lineage in distinct ways in response to the two stimuli. The fact that *PIF4* is highly induced by elevated temperature [8, 24, 32] and only accumulates in meristemoids upon high-temperature treatment (Figure 3A) may provide an explanation for its specific role in regulating the stomatal response toward high temperature.

Arabidopsis plants grown at high temperature display a syndrome of responses, including elongated petioles and elevated leaves (thermonasty), that have been shown to enhance plant cooling [5, 8]. By contrast, reducing stomatal density in response to high temperature, as shown in this study, is expected to decrease plant cooling. This apparent paradox may reflect the complex trade-off that plants need to make in hot weather: increased cooling by transpiration must be balanced against excessive water loss, particularly because hot conditions often coincide with drought. Strikingly, both thermonasty and stomatal density are controlled by PIF4, indicating the central role of this transcription factor in coordinating these responses to complex environmental cues. The response of stomatal development in plants to temperature is complex and likely influenced by both the local environment and, in the case of crops, artificial selection [42]. It will be interesting to determine whether the PIF4-SPCH regulatory module is conserved in other species and whether its behavior mirrors the different phenotypic responses to high temperature.

STAR★METHODS

CONTACT FOR REAGENT AND RESOURCE SHARING

Further information and requests for resources and reagents should be directed to and will be fulfilled by the Lead Contact, On Sun Lau (onsunlau@nus.edu.sg).

EXPERIMENTAL MODEL AND SUBJECT DETAILS

Plant materials and growth conditions—The *Arabidopsis* ecotype Columbia-0 (Col) was used as the wild-type control in all experiments. The following transgenic lines and mutants employed in the study were reported previously: *SPCHpro:nucGFP* [6]; *SPCHpro:SPCH-YFP* [19], *SPCHpro:SPCH2-4A-YFP* [14]; *pif4* [43]; *pif4-2* [28]; *PIF4-OX* and *PIF4pro:PIF4-MYC* in *pifq* [32]. Seedling were grown on ½ strength Murashige and Skoog (MS) agar media (1%) at the indicated temperature in environmental control

chambers (Percival) at a light intensity of ~70 μmol m^{-2} s^{-1}. The relative low light intensity facilitates high temperature responses [13, 48]. In most experiments, seedlings were grown under long-day (16h-light/8h-dark) conditions. Short-day conditions (8h-light/16h-dark) were used for the experiment in Figure 2B. For experiments that involves a temperature shift, the shift was carried out at Zeitgeber Time 0 and samples were collected after incubation of the indicated time.

Accession numbers—Sequence information of the genes studied in this article can be obtained from The *Arabidopsis* Information Resource (TAIR) (http://www.arabidopsis.org) with the following accession numbers: *SPCH*, AT5G53210; *PIF4*, AT2G43010; *ICE1*, AT3G26744; *TMM*, AT1G80080; *ERL1*, AT5G62230.

METHOD DETAILS

Vector construction and plant transformation—*ATML1pro:GR-SPCH1-4A-YFP* (Dexamethasone-inducible SPCH) was generated by amplifying the glucorticoid receptor (GR) with added NotI sites from pJAN33-FLAG:GR (gift of Stephen Wenkel) with primers GCG GCC GC ATG GAA GCT CGA AAA ACA AAG AA and GCG GCC GC TTT TTG ATG AAA CAG AAG CTT TTT G, subcloning into pJET (Fermentas), and then digesting and ligating into pENTR-SPCH1-4A. *ATML1pro* was amplified from pAR169 ATML1p:mCitrine-RCI2A (gift of Adrienne Roeder) [18, 19, 49] with GGGG ACA ACT TTG TAT AGA AAA GTT G AAG CTT ATC AAA GAA AAA AC and GGGG AC TGC TTT TTT GTA CAA ACT TG TAA CCG GTG GAT TCA GGG, subcloned into pJET (Fermentas) then recombined into pDONR with BP Clonase II (Thermo Fisher Scientific). pDONR-ATML1pro and pENTR-GR-SPCH1-4A were then recombined into R4pGWB540 [32, 44] using LR Clonase II (Thermo Fisher Scientific).

To construct *PIF4pro:PIF4-GFP*, a *PIF4*-containing genomic fragment was amplified from genomic DNA using primers CACC GCC TGT TTA ATT GGT GCT TGG TCA ATT ACG (forward) and GTG GTC CAA ACG AGA ACC GTC GGT GGT CT (reverse). These amplified the 4.3 kb upstream of the ATG of *PIF4* and its whole coding region with introns, missing the termination codon. This PCR product was cloned into pENTR (Thermo Fisher Scientific). The pENTR clone was checked with sequencing and recombined with the binary vector containing GFP (pJHA212-GFP-gateway) using Gateway cloning (Thermo Fisher Scientific).

The binary vectors were transformed into Col (for *ATML1pro:GR-SPCH1-4A-YFP*) or *pif4-101* [22, 50] (for *PIF4pro:PIF4-GFP*) using the floral-dip method [6, 51] and transgenic plants were selected on antibiotic-containing ½ MS agar plates.

Analysis of transcriptional and translational reporters and the stomatal phenotype of mutants—For confocal microscopy, fluorescence images were captured on a Leica SP5, a Leica SP8 (both equipped with a Hybrid detector) or an Olympus FV3000 microscope and were processed with ImageJ (National Institutes of Health). Deconvolution of the PIF4-GFP images (Figure 3) were carried out by the image processing software Huygens Professional (Scientific Volume Imaging). Cell outlines were visualized with propidium iodide (Molecular Probes, P3566; 0.1 mg/ml). Quantitation of fluorescence

intensity was performed using ImageJ by marking the nuclear signals as region of interests (ROIs) and measuring their intensity with its built-in tools.

For quantification of stomatal phenotypes, seedlings were first cleared in 7:1 ethanol:acetic acid solution and mounted in Hoyer's medium. For a given genotype, differential contrast interference (DIC) images of the abaxial epidermis of cotyledons were captured at 20X on a Zeiss AxioImager M2 or a Leica DM2500 microscope (0.441 or 0.320 mm^{-2} field of view, respectively). More than 15 cotyledons were examined per test.

RT-qPCR experiments—Total RNA from seedlings was purified using RNeasy Plant Mini Kit with DNaseI digestion (QIAGEN). Seven hundred ng of the RNA was used in reverse transcription using the iScript cDNA synthesis kit (Bio-Rad). Quantitative PCR were performed with gene specific primers (Table S2; designed with QuantPrime [19, 52]) and the SsoAdvanced SYBR Green Supermix (Bio-Rad) on a CFX96 Real-Time PCR detection system (Bio-Rad). Relative expression of target genes in the different samples was calculated from *ACTIN2- or PP2A*-normalized target signals using the Δ^{CT} method.

Chromatin Immunoprecipitation (ChIP) assays—Seven-day-old seedlings of *PIF4pro:PIF4-MYC* (in *pifq*) and Col were grown at the indicated temperature and were transferred to 28°C for 4 h or not before harvested. ChIPs were carried out based on standard protocol [14, 53] (Figure S3) or our MOBE-ChIP method [13, 34, 43, 54, 55] (Figure 3E). For MOBE-ChIP, briefly, a substantially larger amount of plant materials was used (~12 g for each sample in this study), but was processed at smaller aliquots before the immunoprecipitation step. Chromatin fragmentation was carried out on a Bioruptor sonicator (Diagenode) with the following settings: 24 High intensity cycles of 30 s "on" and 30 s "off" at 4°C. Immunoprecipitation was carried out at 4°C overnight on a rotating plateform using the monoclonal anti-MYC antibody 71D10 (Cell Signaling Technology). Dynabeads Protein A magnetic beads (Invitrogen) (1h incubation) was used to capture the precipitated complex. Reverse cross-linking of the immunoprecipitated complex was carried out overnight at 65°C and purified by the ChIP DNA Clean & Concentrator (Zymo). Subsequent quantitative PCR reactions were performed with Ssofast EvaGreen Supermix (Bio-Rad) on a CFX96 Real-Time PCR detection system (Bio-Rad) using primers specific to the promoter of *SPCH* or other specified regions (Table S2). Signals from the ChIPed DNA were normalized to their input DNA.

SPCH induction and RNA extraction for RNA-seq—Transgenic lines homozygous for *ATML1pro:GR-SPCH1-4A-YFP* and the Col control were sterilized and cold treated for two days. Seeds were germinated in liquid MS culture medium supplemented with 1% sucrose on a rotating platform (90 rpm). At 7 dpg, seedlings were treated with 100 μM dexamethasone solution (diluted from stock in ethanol) to induce the translocation of GR-SCPH1-4A to the nucleus. Four replicates were collected at 0 (un-treated) and 12 hr post treatment. Total RNA from the seedlings was extracted using RNeasy Plant Mini Kit with DNaseI digestion (QIAGEN). Quality of the RNA samples was assessed with a 2100 Bioanalyzer (Agilent).

RNA-seq library preparation, high-throughput sequencing and data analysis— Barcoded mRNA libraries were constructed by using the Illumina Poly-A Purification TruSeq library kit (performed by Duke University's Genomics Core Facility). Samples were sequenced on Illumina HiSeq 2000 (single-read 50-bp run) with the 16 RNA samples multiplexed on two lanes (8 samples/lane). RNA-seq analyses were performed as described [13, 28]. Briefly, Tophat [32, 45] was used to align reads to the TAIR 10 genome assembly with default parameters. Multi-mapped or unmapped reads were filtered using Samtools. To generate count data, reads mapped to gene features were summarized using HTSeq [46]. DESeq [47] was used to determine differential expression between SPCH induction samples and WT, implementing an interaction test in the analytical design between genotype and induction time. Adjusting via the Benjamini & Hochberg method, differentially expressed genes with FDR < 0.05 were called significant.

QUANTIFICATION AND STATISTICAL ANALYSIS

Statistical analyses were performed using Microsoft Excel, GraphPad Prism version 6 or through an online website (http://astatsa.com/OneWay_Anova_with_TukeyHSD/). Details of the statistical tests applied, including the statistical methods, number of replicates, mean and error bar details and significances, are indicated in the relevant figure legends. All replicates are biological, unless otherwise noted in the figure legend.

DATA AND SOFTWARE AVAILABILITY

RNA-seq data are available under accession number GEO: GSE110302.

Supplementary Material

Refer to Web version on PubMed Central for supplementary material.

Acknowledgments

We thank Z.-Y. Wang, G. Choi, E. Oh, and P. Quail for *Arabidopsis* mutants and transgenic lines and members of our laboratories for critical comments. Funding for this work was provided by Academic Research Fund (MOE2017-T2-1-017) from the Ministry of Education - Singapore, intramural research fund (R-154-000-A16-114) from the National University of Singapore to O.S.L., and NIH 1R01GM086632 to D.C.B. Z.S. is supported by the China Scholarship Council, K.A.D. was supported by a graduate research fellowship (NSF) and the Cellular and Molecular Biology Training Program (NIH5T32GM007276), and D.L. was supported by an Erwin Schroedinger Fellowship from the Austrian Science Fund FWF. O.S.L. was a Croucher Fellow, and D.C.B. is an Investigator of the Howard Hughes Medical Institute.

References

1. Lau OS, Bergmann DC. Stomatal development: a plant's perspective on cell polarity, cell fate transitions and intercellular communication. Development. 2012; 139:3683–3692. [PubMed: 22991435]
2. Han S-K, Torii KU. Lineage-specific stem cells, signals and asymmetries during stomatal development. Development. 2016; 143:1259–1270. [PubMed: 27095491]
3. Casson SA, Hetherington AM. Environmental regulation of stomatal development. Curr Opin Plant Biol. 2010; 13:90–95. [PubMed: 19781980]
4. IPCC. Climate Change 2014: Synthesis Report. In: Pachauri, RK., Meyer, LA., editors. Contribution of Working Groups I, II and III to the Fifth Assessment Report of the Intergovernmental Panel on Climate Change. IPCC; 2014.

5. Crawford AJ, McLachlan DH, Hetherington AM, Franklin KA. High temperature exposure increases plant cooling capacity. Curr Biol. 2012; 22:R396–R397. [PubMed: 22625853]
6. MacAlister CA, Ohashi-Ito K, Bergmann DC. Transcription factor control of asymmetric cell divisions that establish the stomatal lineage. Nature. 2007; 445:537–540. [PubMed: 17183265]
7. Pillitteri LJ, Sloan DB, Bogenschutz NL, Torii KU. Termination of asymmetric cell division and differentiation of stomata. Nature. 2007; 445:501–505. [PubMed: 17183267]
8. Koini MA, Alvey L, Allen T, Tilley CA, Harberd NP, Whitelam GC, Franklin KA. High temperature-mediated adaptations in plant architecture require the bHLH transcription factor PIF4. Curr Biol. 2009; 19:408–413. [PubMed: 19249207]
9. Quint M, Delker C, Franklin KA, Wigge PA, Halliday KJ, van Zanten M. Molecular and genetic control of plant thermomorphogenesis. Nat Plants. 2016; 2:15190. [PubMed: 27250752]
10. Kumar SV, Lucyshyn D, Jaeger KE, Alós E, Alvey E, Harberd NP, Wigge PA. Transcription factor PIF4 controls the thermosensory activation of flowering. Nature. 2012; 484:242–245. [PubMed: 22437497]
11. Radin JW, Lu Z, Percy RG, Zeiger E. Genetic variability for stomatal conductance in Pima cotton and its relation to improvements of heat adaptation. Proc Natl Acad Sci USA. 1994; 91:7217–7221. [PubMed: 11607487]
12. Berry JA, Beerling DJ, Franks PJ. Stomata: key players in the earth system, past and present. Curr Opin Plant Biol. 2010; 13:233–240. [PubMed: 20552724]
13. Lau OS, Davies KA, Chang J, Adrian J, Rowe MH, Ballenger CE, Bergmann DC. Direct roles of SPEECHLESS in the specification of stomatal self-renewing cells. Science. 2014; 345:1605–1609. [PubMed: 25190717]
14. Lampard GR, Macalister CA, Bergmann DC. Arabidopsis stomatal initiation is controlled by MAPK-mediated regulation of the bHLH SPEECHLESS. Science. 2008; 322:1113–1116. [PubMed: 19008449]
15. Kim T-W, Michniewicz M, Bergmann DC, Wang Z-Y. Brassinosteroid regulates stomatal development by GSK3-mediated inhibition of a MAPK pathway. Nature. 2012; 482:419–422. [PubMed: 22307275]
16. Gudesblat GE, Schneider-Pizoń J, Betti C, Mayerhofer J, Vanhoutte I, van Dongen W, Boeren S, Zhiponova M, de Vries S, Jonak C, Russinova E. SPEECHLESS integrates brassinosteroid and stomata signalling pathways. Nat Cell Biol. 2012; 14:548–554. [PubMed: 22466366]
17. Kumari A, Jewaria PK, Bergmann DC, Kakimoto T. Arabidopsis reduces growth under osmotic stress by decreasing SPEECHLESS protein. Plant Cell Physiol. 2014; 55:2037–2046. [PubMed: 25381317]
18. Adrian J, Chang J, Ballenger CE, Bargmann BOR, Alassimone J, Davies KA, Lau OS, Matos JL, Hachez C, Lanctot A, et al. Transcriptome dynamics of the stomatal lineage: birth, amplification, and termination of a self-renewing population. Dev Cell. 2015; 33:107–118. [PubMed: 25850675]
19. Matos JL, Lau OS, Hachez C, Cruz-Ramírez A, Scheres B, Bergmann DC. Irreversible fate commitment in the Arabidopsis stomatal lineage requires a FAMA and RETINOBLASTOMA-RELATED module. eLife. 2014; 3:e03271.
20. Leivar P, Quail PH. PIFs: pivotal components in a cellular signaling hub. Trends Plant Sci. 2011; 16:19–28. [PubMed: 20833098]
21. Al-Sady B, Ni W, Kircher S, Schäfer E, Quail PH. Photoactivated phytochrome induces rapid PIF3 phosphorylation prior to proteasome-mediated degradation. Mol Cell. 2006; 23:439–446. [PubMed: 16885032]
22. Lorrain S, Allen T, Duek PD, Whitelam GC, Fankhauser C. Phytochrome-mediated inhibition of shade avoidance involves degradation of growth-promoting bHLH transcription factors. Plant J. 2008; 53:312–323. [PubMed: 18047474]
23. Ni W, Xu S-L, Tepperman JM, Stanley DJ, Maltby DA, Gross JD, Burlingame AL, Wang ZY, Quail PH. A mutually assured destruction mechanism attenuates light signaling in Arabidopsis. Science. 2014; 344:1160–1164. [PubMed: 24904166]
24. Foreman J, Johansson H, Hornitschek P, Josse E-M, Fankhauser C, Halliday KJ. Light receptor action is critical for maintaining plant biomass at warm ambient temperatures. Plant J. 2011; 65:441–452. [PubMed: 21265897]

25. Jung J-H, Domijan M, Klose C, Biswas S, Ezer D, Gao M, Khattak AK, Box MS, Charoensawan V, Cortijo S, et al. Phytochromes function as thermosensors in Arabidopsis. Science. 2016; 354:886–889. [PubMed: 27789797]
26. Legris M, Klose C, Burgie ES, Rojas CCR, Neme M, Hiltbrunner A, Wigge PA, Schäfer E, Vierstra RD, Casal JJ. Phytochrome B integrates light and temperature signals in Arabidopsis. Science. 2016; 354:897–900. [PubMed: 27789798]
27. Shen Y, Zhou Z, Feng S, Li J, Tan-Wilson A, Qu L-J, Wang H, Deng XW. Phytochrome A mediates rapid red light-induced phosphorylation of Arabidopsis FAR-RED ELONGATED HYPOCOTYL1 in a low fluence response. Plant Cell. 2009; 21:494–506. [PubMed: 19208901]
28. Leivar P, Monte E, Al-Sady B, Carle C, Storer A, Alonso JM, Ecker JR, Quail PH. The Arabidopsis phytochrome-interacting factor PIF7, together with PIF3 and PIF4, regulates responses to prolonged red light by modulating phyB levels. Plant Cell. 2008; 20:337–352. [PubMed: 18252845]
29. Nozue K, Covington MF, Duek PD, Lorrain S, Fankhauser C, Harmer SL, Maloof JN. Rhythmic growth explained by coincidence between internal and external cues. Nature. 2007; 448:358–361. [PubMed: 17589502]
30. Yamashino T, Nomoto Y, Lorrain S, Miyachi M, Ito S, Nakamichi N, Fankhauser C, Mizuno T. Verification at the protein level of the PIF4-mediated external coincidence model for the temperature-adaptive photoperiodic control of plant growth in Arabidopsis thaliana. Plant Signal Behav. 2013; 8:e23390. [PubMed: 23299336]
31. Casson SA, Hetherington AM. Phytochrome B is required for light-mediated systemic control of stomatal development. Curr Biol. 2014; 24:1216–1221. [PubMed: 24835461]
32. Oh E, Zhu J-Y, Wang Z-Y. Interaction between BZR1 and PIF4 integrates brassinosteroid and environmental responses. Nat Cell Biol. 2012; 14:802–809. [PubMed: 22820378]
33. Amoutzias GD, Robertson DL, Van de Peer Y, Oliver SG. Choose your partners: dimerization in eukaryotic transcription factors. Trends Biochem Sci. 2008; 33:220–229. [PubMed: 18406148]
34. Lau OS, Bergmann DC. MOBE-ChIP: a large-scale chromatin immunoprecipitation assay for cell type-specific studies. Plant J. 2015; 84:443–450. [PubMed: 26332947]
35. Franklin KA, Lee SH, Patel D, Kumar SV, Spartz AK, Gu C, Ye S, Yu P, Breen G, Cohen JD, et al. Phytochrome-interacting factor 4 (PIF4) regulates auxin biosynthesis at high temperature. Proc Natl Acad Sci USA. 2011; 108:20231–20235. [PubMed: 22123947]
36. Lafos M, Kroll P, Hohenstatt ML, Thorpe FL, Clarenz O, Schubert D. Dynamic regulation of H3K27 trimethylation during Arabidopsis differentiation. PLoS Genet. 2011; 7:e1002040. [PubMed: 21490956]
37. Zhang Y, Mayba O, Pfeiffer A, Shi H, Tepperman JM, Speed TP, Quail PH. A quartet of PIF bHLH factors provides a transcriptionally centered signaling hub that regulates seedling morphogenesis through differential expression-patterning of shared target genes in Arabidopsis. PLoS Genet. 2013; 9:e1003244. [PubMed: 23382695]
38. Sessions A, Weigel D, Yanofsky MF. The Arabidopsis thaliana MERISTEM LAYER 1 promoter specifies epidermal expression in meristems and young primordia. Plant J. 1999; 20:259–263. [PubMed: 10571886]
39. Zhu J-Y, Sae-Seaw J, Wang Z-Y. Brassinosteroid signalling. Development. 2013; 140:1615–1620. [PubMed: 23533170]
40. Arabidopsis Interactome Mapping Consortium. Evidence for network evolution in an Arabidopsis interactome map. Science. 2011; 333:601–607. [PubMed: 21798944]
41. Casson SA, Franklin KA, Gray JE, Grierson CS, Whitelam GC, Hetherington AM. phytochrome B and PIF4 regulate stomatal development in response to light quantity. Curr Biol. 2009; 19:229–234. [PubMed: 19185498]
42. Jumrani K, Bhatia VS, Pandey GP. Impact of elevated temperatures on specific leaf weight, stomatal density, photosynthesis and chlorophyll fluorescence in soybean. Photosynth Res. 2017; 131:333–350. [PubMed: 28025729]
43. Shin J, Kim K, Kang H, Zulfugarov IS, Bae G, Lee C-H, Lee D, Choi G. Phytochromes promote seedling light responses by inhibiting four negatively-acting phytochrome-interacting factors. Proc Natl Acad Sci USA. 2009; 106:7660–7665. [PubMed: 19380720]

44. Nakagawa T, Nakamura S, Tanaka K, Kawamukai M, Suzuki T, Nakamura K, Kimura T, Ishiguro S. Development of R4 gateway binary vectors (R4pGWB) enabling high-throughput promoter swapping for plant research. Biosci Biotechnol Biochem. 2008; 72:624–629. [PubMed: 18256458]
45. Trapnell C, Pachter L, Salzberg SL. TopHat: discovering splice junctions with RNA-seq. Bioinformatics. 2009; 25:1105–1111. [PubMed: 19289445]
46. Anders S, Pyl PT, Huber W. HTSeq–a Python framework to work with high-throughput sequencing data. Bioinformatics. 2015; 31:166–169. [PubMed: 25260700]
47. Anders S, Huber W. Differential expression analysis for sequence count data. Genome Biol. 2010; 11:R106. [PubMed: 20979621]
48. Delker C, Sonntag L, James GV, Janitza P, Ibañez C, Ziermann H, Peterson T, Denk K, Mull S, Ziegler J, et al. The DET1-COP1-HY5 pathway constitutes a multipurpose signaling module regulating plant photomorphogenesis and thermomorphogenesis. Cell Rep. 2014; 9:1983–1989. [PubMed: 25533339]
49. Roeder AHK, Chickarmane V, Cunha A, Obara B, Manjunath BS, Meyerowitz EM. Variability in the control of cell division underlies sepal epidermal patterning in Arabidopsis thaliana. PLoS Biol. 2010; 8:e1000367. [PubMed: 20485493]
50. Kanaoka MM, Pillitteri LJ, Fujii H, Yoshida Y, Bogenschutz NL, Takabayashi J, Zhu JK, Torii KU. SCREAM/ICE1 and SCREAM2 specify three cell-state transitional steps leading to arabidopsis stomatal differentiation. Plant Cell. 2008; 20:1775–1785. [PubMed: 18641265]
51. Clough SJ. Floral dip: agrobacterium-mediated germ line transformation. Methods Mol Biol. 2005; 286:91–102. [PubMed: 15310915]
52. Arvidsson S, Kwasniewski M, Riaño-Pachón DM, Mueller-Roeber B. QuantPrime–a flexible tool for reliable high-throughput primer design for quantitative PCR. BMC Bioinformatics. 2008; 9:465. [PubMed: 18976492]
53. Gendrel A-V, Lippman Z, Martienssen R, Colot V. Profiling histone modification patterns in plants using genomic tiling microarrays. Nat Methods. 2005; 2:213–218. [PubMed: 16163802]
54. Lau OS. Characterization of cell-type-specific DNA binding sites of plant transcription factors using chromatin immunoprecipitation. Methods Mol Biol. 2017; 1629:37–45. [PubMed: 28623578]
55. Wang S, Lau OS. MOBE-ChIP: probing cell type-specific binding through large-scale chromatin immunoprecipitation. Methods Mol Biol. 2018; 1689:167–176. [PubMed: 29027174]

In Brief

Lau et al. report a mechanism underlying suppression of stomatal production in response to higher temperatures. In warmth, PIF4 accumulates in stomatal precursors and directly represses *SPCH*, the master initiator of stomatal development. This work highlights how an environmental cue and broadly expressed regulator control a specific cell lineage.

Highlights

- In warmer temperatures, *Arabidopsis* produces fewer stomata and expresses less *SPCH*
- PIF4 is important in the elevated-temperature-dependent stomatal response
- Warm temperature induces PIF4 in stomatal precursors, which suppresses *SPCH* directly
- SPCH feeds back negatively on *PIF4* by directly repressing its expression

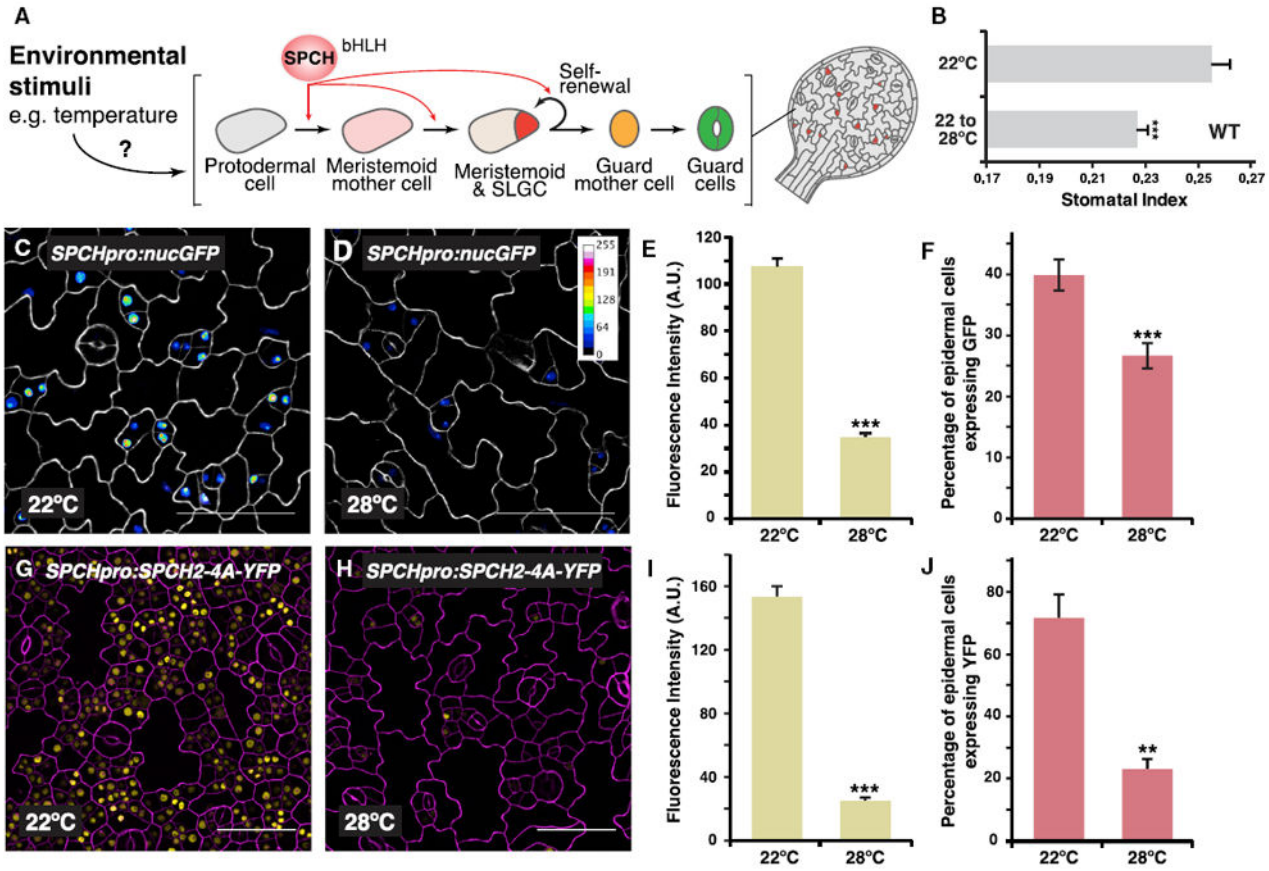

Figure 1. High Temperature Suppresses Stomatal Development and *SPCH* Expression

(A) Schematic of stomatal development in *Arabidopsis*. SPCH controls the initiation and proliferation of the self-renewing stomatal precursors and is a prime target for environmental control of the lineage.

(B) Quantification of effects of high temperature on stomatal indices (the ratio of stomata to total epidermal cells) in wild-type (WT) abaxial cotyledons (14 dpg). Seedlings were either grown at 22°C continuously or transferred to 28°C after 4 days.

(C–F) Analysis of a transcriptional reporter of *SPCH*. Confocal images of 3-day-old abaxial cotyledons of *SPCHpro:nucGFP* grown at either 22°C (C) or 28°C (D) are shown. Fluorescence intensity of the GFP channel is indicated in the calibration bar and as signal intensity (E). In (F), the percentage of GFP-expressing cells over total epidermal cells in an area is quantified. Images were taken with the same excitation and acquisition settings.

(G–J) Analysis of a MAPK-insensitive translational reporter of SPCH. Confocal images of 3-day-old abaxial cotyledons of *SPCHpro:SPCH2-4A-YFP* (yellow) grown at either 22°C (G) or 28°C (H) are shown. Fluorescence intensity (I) and numbers (J; as percentage of total epidermal cells) of YFP-expressing cells are quantified.

Values are mean ± SEM; ≥ 20 (B), 30 (E and I), 10 (F), and 4 (J). Student's t test; ***$p < 0.001$; **$p < 0.01$. Cell outlines were visualized with propidium iodide (C and D, white; G and I, magenta). The scale bar represents 50 μm. See also Figure S1.

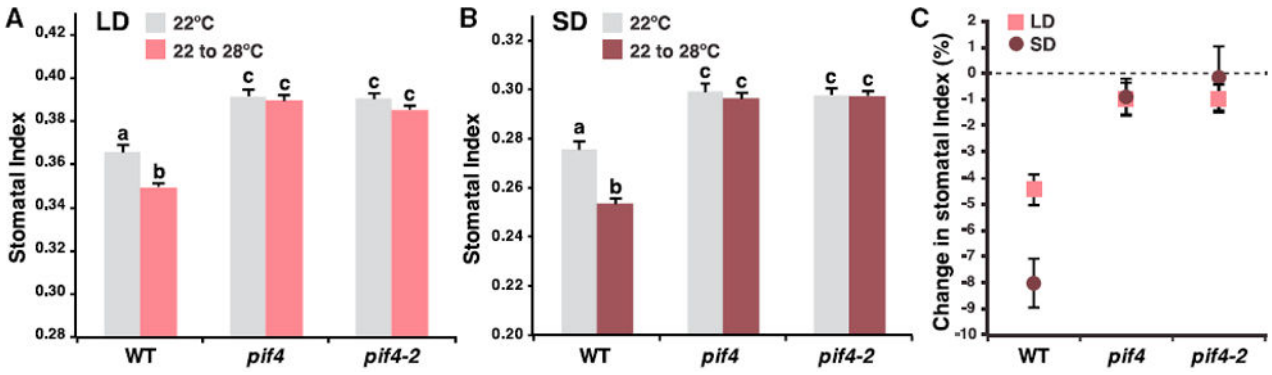

Figure 2. PIF4 Is Involved in High-Temperature Regulation of Stomatal Development

(A and B) Quantification of effects of high temperature on stomatal indices in WT and *pif4* mutant (*pif4* and *pif4-2*) abaxial cotyledons under long-day (LD; A) or short-day (SD; B) conditions. Plants were grown at 22°C for 4 days before transfer to 28°C for 10 (LD, red) or 23 (SD, maroon) more days. At these respective time points, plants were at similar developmental stage with six leaves. Controls were maintained at 22°C (gray).

(C) Changes in stomatal indices in response to high temperature in WT, *pif4*, and *pif4-2* under LD (red) and SD (maroon) conditions (data derived from A and B). Shown are percentage changes from the "22°C–28°C" samples relative to samples grown at 22°C. (A and B) Values are mean ± SEM; ≥ 20. One-way ANOVA with post hoc Tukey HSD; $p < 0.01$. See also Figure S2.

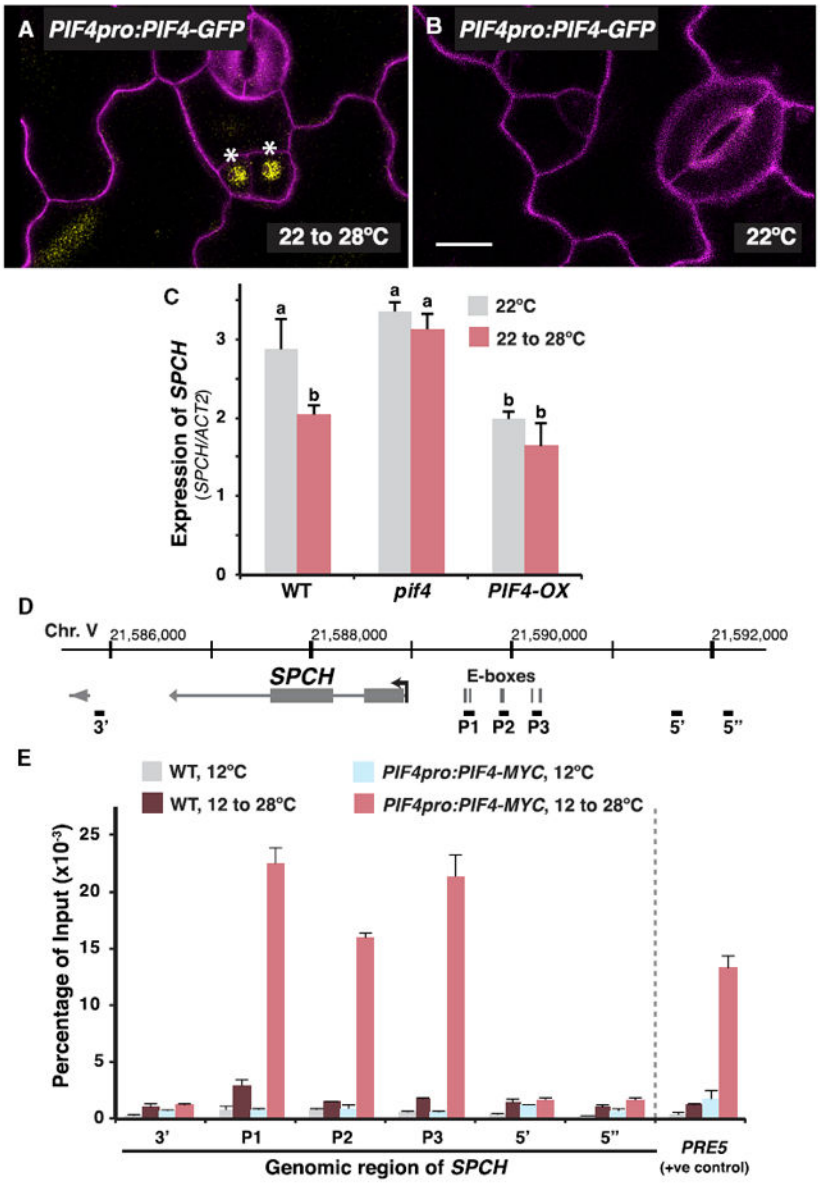

Figure 3. PIF4 Binds to *SPCH* Promoter in a Temperature-Dependent Manner and Regulates *SPCH* Expression

(A and B) Stomatal lineage expression pattern of a translational reporter of *PIF4*. Confocal analysis of 3-day-old abaxial cotyledons of *PIF4pro:PIF4-GFP* (yellow) is shown. Plants were grown at 22°C before transfer to 28°C for 16 hr (A) or not (B). Cell outlines (magenta) were stained with propidium iodide. Asterisks marked stomatal lineage cells with GFP expression. The scale bar represents 10 μm.

(C) Gene expression analysis of *SPCH* in WT, *pif4*, and a PIF4-overexpressing line (*PIF4-OX*) by qRT-PCR. RNA was extracted from 3-day-old seedlings that were grown at 22°C and were transferred to 28°C for 8 hr before harvest (red). Control plants were maintained at 22°C (gray). Values are mean ± SEM; n = 4. One-way ANOVA with post hoc Tukey HSD; $p < 0.01$.

(D) Gene structure of *SPCH*. Arrow marks the transcription start site (TSS) and gene orientation. Grey vertical bars denote position of E-boxes (2 kbp upstream of the TSS only). Black horizontal bars indicate the regions tested by ChIP-qPCR in (E).
(E) MOBE-ChIP-qPCR assays were performed on WT and *PIF4pro:PIF4-MYC* using an anti-Myc antibody. Plants were grown for 7 days at 12°C before transferred to 28°C for 4 hr or kept at 12°C. Various genomic regions of *SPCH* were tested, as shown in (D). *PRE5*, a known target of PIF4, was used as a positive control [32]. Values are mean ± SEM (technical replicates); n = 3. Assay was repeated with similar results.
See also Figure S3.

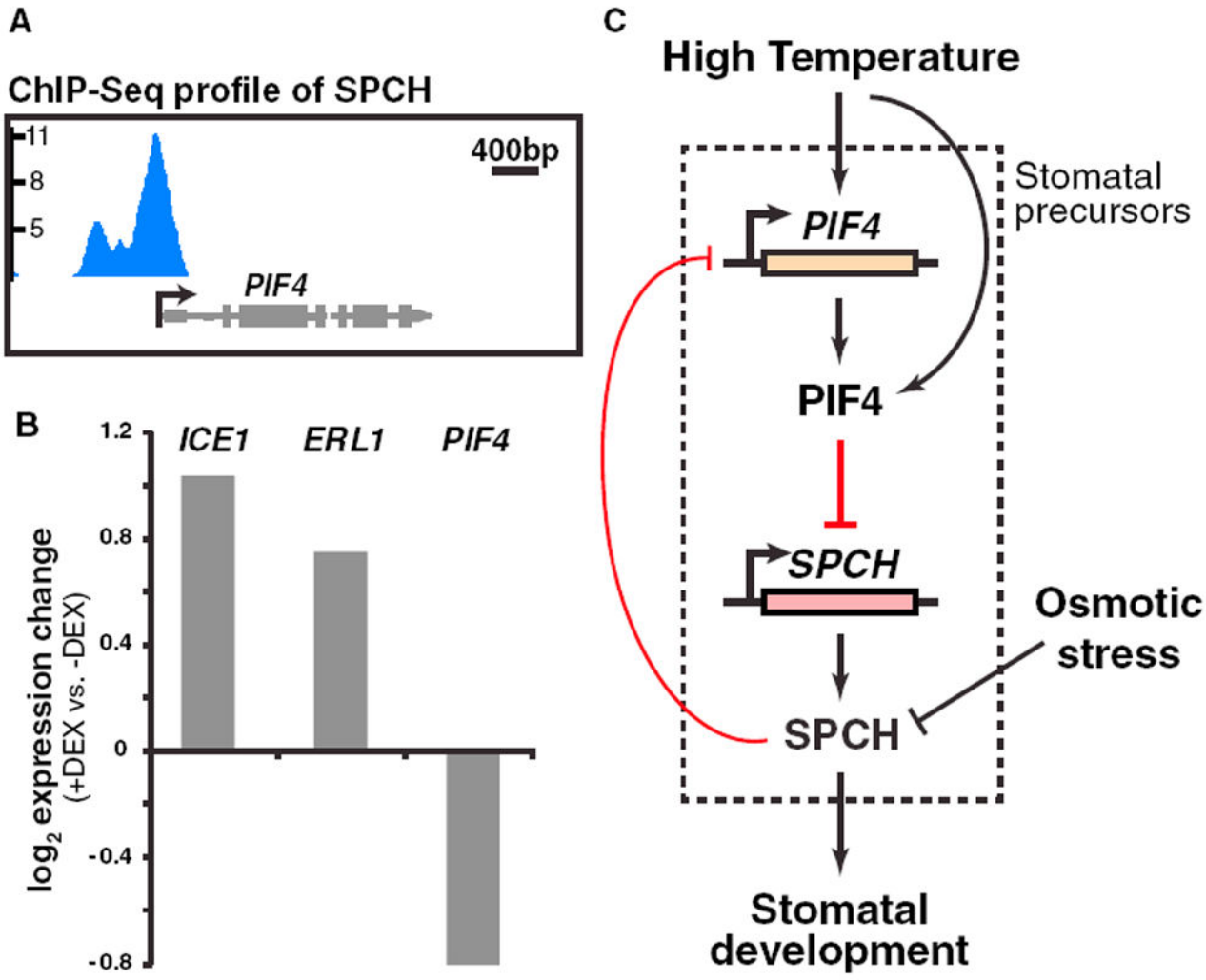

Figure 4. SPCH Directly Binds and Regulates *PIF4*

(A) ChIP-seq profile of SPCH binding at the *PIF4* locus. Data are derived from [13].

(B) Expression changes of the indicated genes upon dexamethasone (DEX) induction (12 hr) of GR-SPCH1-4A in leaf epidermis derived from RNA-seq analysis.

(C) Model of the regulatory interplay between *SPCH* and *PIF4* in the high-temperature regulation of stomatal development. At high temperature, *PIF4* is induced and accumulates in the stomatal precursors, where it binds and represses *SPCH* to inhibit activity of the stomatal lineage. In the few cells where SPCH accumulates, it negatively feeds back on *PIF4* through direct binding of *PIF4*'s promoter, enabling SPCH to accumulate sufficiently to ensure stomatal cell fate. Other environmental signals, such as osmotic stress, influence *SPCH* at the protein level through the MAPK pathway (not shown).

See also Figure S4.

KEY RESOURCES TABLE

REAGENT or RESOURCE	SOURCE	IDENTIFIER
Antibodies		
Rabbit monoclonal anti-Myc	Cell Signaling Technology	Cat#2278S; RRID: AB_10693332
Bacterial and Virus Strains		
E. coli DH5α	N/A	N/A
A. tumefaciens GV3101	N/A	N/A
Chemicals, Peptides, and Recombinant Proteins		
Propidium Iodide	Molecular Probes	Cat#P3566
Dynabeads Protein A magnetic beads	ThermoFisher Scientific	Cat#10002D
Critical Commercial Assays		
pENTR/D-TOPO Cloning Kit	ThermoFisher Scientific	Cat#K240020
Gateway LR Clonase II Enzyme mix	ThermoFisher Scientific	Cat#11791020
RNeasy Plant Mini Kit	QIAGEN	Cat#74904
iScript cDNA synthesis kit	Bio-Rad	Cat#1708891
SsoAdvanced SYBR Green Supermix	Bio-Rad	Cat#1725271
ChIP DNA Clean & Concentrator	Zymo Research	Cat#D5205
Deposited Data		
RNA-Seq data	This paper	GEO: GSE110302
Experimental Models: Organisms/Strains		
Arabidopsis: Col-0	N/A	N/A
Arabidopsis: SPCHpro:nucGFP	[6]	N/A
Arabidopsis: SPCHpro:SPCH-YFP	[19]	N/A
Arabidopsis: SPCHpro:SPCH2-4A-YFP	[14]	N/A
Arabidopsis: pif4	[43]	N/A
Arabidopsis: pif4-2	[28]	N/A
Arabidopsis: PIF4-OX	[32]	N/A
Arabidopsis: PIF4pro:PIF4-MYC in *pifq*	[32]	N/A
Arabidopsis: ATML1pro:GR-SPCH1-4A-YFP	This study	N/A
Arabidopsis: PIF4pro:PIF4-GFP	This study	N/A
Oligonucleotides		
See Table S2	N/A	N/A
Recombinant DNA		
R4pGWB540	[32, 44]	N/A
ATML1pro:GR-SPCH1-4A-YFP	This study	N/A
PIF4pro:PIF4-GFP	This study	N/A
Software and Algorithms		
Excel	Microsoft	N/A
Prism	GraphPad	N/A
Huygens Professional	Scientific Volume Imaging	N/A

REAGENT or RESOURCE	SOURCE	IDENTIFIER
Tophat	[32, 45]	N/A
HTSeq	[46]	N/A
DESeq	[47]	N/A